Optics Letters

Influence of air humidity on 248-nm ultraviolet laser pulse filamentation

Alexey V. Shutov,[1,*] Daria V. Mokrousova,[1] Vladimir Yu. Fedorov,[1,2] Leonid V. Seleznev,[1] Georgy E. Rizaev,[1] Anna V. Shalova,[3] Vladimir D. Zvorykin,[1] Stelios Tzortzakis,[2,4,5] and Andrey A. Ionin[1]

[1]P.N. Lebedev Physical Institute of the Russian Academy of Sciences, 53 Leninskiy Prospekt, 119991 Moscow, Russia
[2]Science Program, Texas A&M University at Qatar, P.O. Box 23874, Doha, Qatar
[3]Skolkovo Institute of Science and Technology (Skoltech), 3 Nobelya Ulitsa, 121205 Moscow, Russia
[4]Institute of Electronic Structure and Laser (IESL), Foundation for Research and Technology—Hellas (FORTH), P.O. Box 1527, GR-71110 Heraklion, Greece
[5]Materials Science and Technology Department, University of Crete, 71003 Heraklion, Greece
*Corresponding author: shutovalexei@gmail.com

Received 19 February 2019; revised 29 March 2019; accepted 1 April 2019; posted 1 April 2019 (Doc. ID 360223); published 17 April 2019

At first glance, the amount of water molecules naturally contained in humid air is negligibly small to affect filamentation of ultrashort laser pulses. However, here we show, both experimentally and numerically, that for ultraviolet laser pulses with 248 nm wavelength this is not true. We demonstrate that with increase of air humidity the plasma channels generated by the ultraviolet laser pulses in air become longer and wider, while the corresponding electron density in humid air can be up to one order of magnitude higher compared to dry air.

https://doi.org/10.1364/OL.44.002165

Laser filamentation is a phenomenon which describes the nonlinear self-trapping of intense ultrashort laser pulses propagating in transparent media. Due to high intensity of the laser field in the core of filaments, the process of filamentation is accompanied by ionization of propagation medium and generation of extended plasma channels [1]. Over the years, laser filamentation has been used in a very broad spectrum of applications, such as broadband remote sensing of the atmosphere, self-compression of laser pulses, generation of terahertz radiation, or even in weather control [1–4].

Though laser filamentation has been observed in various gaseous and condensed media, the majority of the experiments (due to their simplicity) are conducted in atmospheric air. While atmospheric air is a mixture of gases, one of its contents is water vapor. However, since the fraction of water molecules in air is very low (no more than 5%), for a long time it was believed that the influence of air humidity on the laser filamentation is negligible. To the best of our knowledge, until now air humidity appeared in the studies of laser filamentation only in the context of dispersion and molecular absorption for mid-infrared laser radiation [5], or as an object for remote detection [6–8]. Of course, there are a number of experiments on filamentation (mainly related to weather control [3]) where atmospheric water appears naturally, e.g., studies of rain and snow formation [9–11], experiments on opening paths in fog [12,13], or investigations of lasing action in water vapor [14]. However, none of them were focused on the influence of air humidity on the filamentation process itself. Nevertheless, in our recent studies we showed that air humidity plays an important role in the ionization of air by ultraviolet (UV) laser pulses with 248 nm wavelength [15,16]. We demonstrated that due to the resonance-enhanced multiphoton ionization (REMPI) process, the ionization cross-section of water molecules at 248 nm is by several orders of magnitude larger than that of oxygen and nitrogen—the two main constituents of air. As a result, in this case, the majority of electron plasma is generated by ionization of water molecules, even if their concentration in air is very small. Thus, taking into account that ionization is one of the main mechanisms in laser filamentation [1], one can expect that air humidity may strongly affect filaments and plasma channels produced by UV laser pulses with 248 nm wavelength. We should note that in previous studies of laser filamentation at 248 nm the influence of air humidity was disregarded [17–21].

In this Letter, we present results of our experiments and numerical simulations on the filamentation of UV laser pulses with 248 nm wavelength in atmospheric air with different humidity. Unlike our previous studies [15] where we tried to avoid any nonlinear propagation effects in order to measure the ionization cross-sections of air components for 248 nm wavelength, here we focus on nonlinear propagation of 248 nm laser pulses in the regime of filamentation. We demonstrate how varying air humidity affects different parameters of filaments and, in particular, show that with increasing humidity the generated plasma channels become longer and wider, while the electron density in humid air can be up to one order of magnitude higher compared to dry air. In addition, we show that, contrary to UV laser pulses, the influence of air humidity on filamentation of NIR laser pulses with 744 nm wavelength is negligible.

For our experiments, we use a Ti:sapphire laser system (Avesta Ltd.), which at 10 Hz repetition rate generates 90 fs

laser pulses with central wavelength of 744 nm and maximum energy per pulse 6 mJ. The third harmonic from this laser system gives us UV laser pulses with 248 nm wavelength and energies up to 200 μJ. Figure 1(a) shows the experimental setup for measurements of the electron density in plasma channels generated during filamentation of laser pulses in air with different humidity. Using a lens with 1 m focal distance, we focus the UV laser pulses and produce filaments that are directed through the photoelectric sensor composed of two tube electrodes separated by a gap of 7 mm. To measure the electron density, we apply a DC electric field of 4 kV/cm to one of the sensor's electrodes (HV) and use an oscilloscope (Tektronix, TDS2024B) to record the resulting electric signal, whose amplitude is proportional to the linear electron density (number of electrons per unit length) integrated over the inter-electrode gap [15,22]. By moving the focusing lens, which is mounted on an optical rail, we record the distribution of the electron density along the plasma channel.

We place the photoelectric sensor inside a sealed gas chamber at a distance of 70 cm behind its input window made of CaF_2. Within the gas chamber we prepare air with three different values of relative humidity (RH): moderate, low, and high. First, we fill the gas chamber with ambient air whose RH vary in the range from 20 to 40%. The initial value of RH depends on the weather conditions, but during the experiment it remains constant. Next, we vacuum pump the gas chamber down to 10^{-2} Torr and then refill it with a mixture of pure nitrogen (80%) and oxygen (20%) passed through a cryogenic trap, which freezes all residual water vapor. Using the above method, we obtain dry air with concentration of water molecules below 0.1 ppm [15], which corresponds to RH = 0%. Finally, in order to prepare air with high RH we fill the gas chamber with ambient air, put a cup of deionized water inside, and seal the chamber overnight. As a result, the next day we obtain humid air with RH exceeding 80%. To monitor the exact values of temperature and RH within the gas chamber, we use a digital thermo-hygrometer (Oregon Scientific, EMR812HGN). During the experiments, the temperature inside the chamber was close to 21°C independently of RH.

We conducted the experiment using UV laser pulses with two different energies, 20 and 50 μJ, which correspond to $P/P_{cr} = 0.8$ and 2, respectively, where P is the peak power and P_{cr} is the critical power of self-focusing. The energy of laser pulses is tuned with the attenuator [see Fig. 1(a)]. Using the vCHIRP software [23], we estimated that due to dispersion in air and optical elements the duration of UV laser pulses after the chamber's entrance window becomes equal to 170–175 fs (FWHM). The measured beam size was equal to 2 mm (FWHM).

Figure 2 shows the experimentally measured dependence of the linear electron density N_e on the propagation distance z for air with three different values of RH. In Figs. 2(a) and 2(b), we see that for UV laser pulses the peak value of electron density $N_{e,\max}$ as well as the total amount of plasma electrons J_e (integral of N_e over z) grow with increase of RH. In particular, for 20 μJ UV laser pulses $N_{e,\max}$ and J_e increase by 11 and 13 times, respectively, when RH changes from 0 to 81%. In turn for UV laser pulses with 50 μJ the change of RH from 0 to 88% results in increase of $N_{e,\max}$ and J_e by 3.7 and 4.8 times, respectively. Additionally, Figs. 2(a) and 2(b) show that in air with higher humidity the plasma channels become longer.

As we have seen, even a small change in fraction of water molecules in air (from 0 to about 2% when RH increases from 0 to about 80–90%) leads to a significant growth of the amount of electrons generated by UV laser pulses. The reason behind this boost of the electrons yield is resonance-enhanced multiphoton ionization (REMPI) of water molecules [15]. For better clarity, Fig. 1(b) shows a sketch of the electronic energy levels in a water molecule. We see that due to the presence of $\tilde{C}^1B_1$ level with energy 10 eV, the UV radiation with 5 eV photon energy (248 nm wavelength) gets into an intermediate two-photon resonance. As a result, instead of regular 3-photon ionization, which goes through virtual intermediate states, we have a much more effective (2 + 1)-photon REMPI. Therefore, despite the fact that the ionization energies of oxygen and water molecules are close (12.06 eV for O_2 and 12.62 eV for H_2O), the ionization of water molecules is much more efficient. Interestingly, one can expect a similar REMPI effect for the fundamental radiation at 744 nm wavelength (or any other laser radiation which covers the 10 eV energy gap of $\tilde{X}^1A_1 \rightarrow \tilde{C}^1B_1$ transition with even number of photons required due to parity conservation).

Indeed, since the total energy of three photons at 744 nm is equal to the energy of one UV photon at 248 nm, the

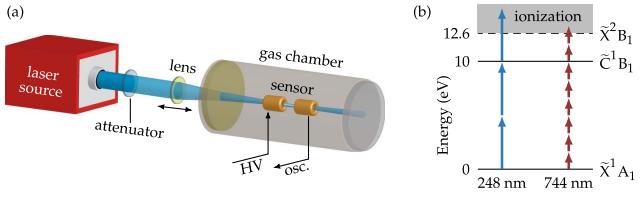

Fig. 1. (a) Experimental setup ("HV"—high-voltage, "osc."—oscilloscope). (b) Sketch of energy levels in a water molecule.

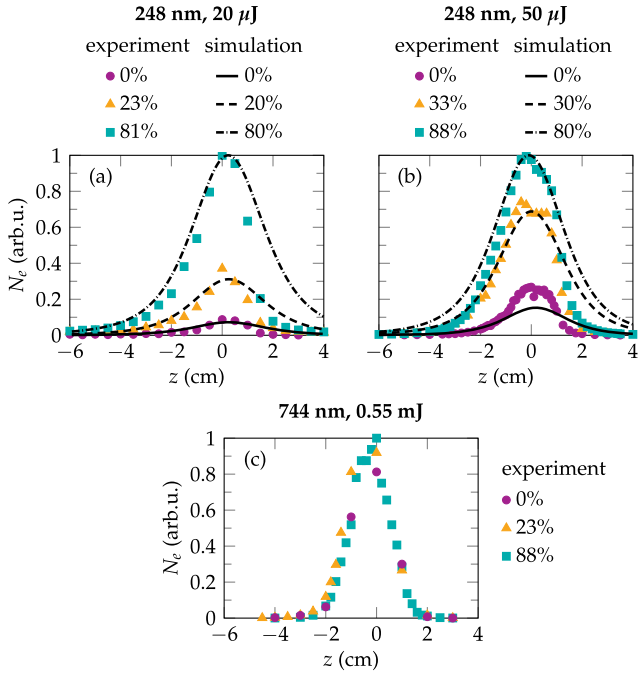

Fig. 2. Linear electron density N_e versus propagation distance z ($z = 0$ corresponds to the lens focus) for different relative humidities. 248 nm laser pulses with energies of (a) 20 μJ and (b) 50 μJ; (c) 744 nm laser pulses with energy of 0.55 mJ. Marks—experimental results; lines—simulation.

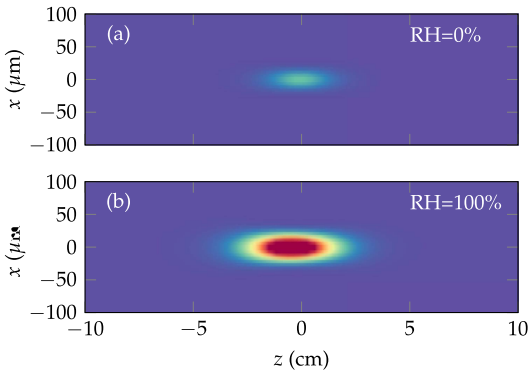

five times higher than for dry air with RH = 0%. In turn, due to the generation of more electrons in air with higher humidity, the losses of laser energy increase with growth of RH—more than twice for 50 μJ UV laser pulses when RH changes from 0 to 100% [Fig. 3(d)]. In total, Fig. 3 shows that in case of 20 μJ pulses with subcritical peak power the change of filamentation parameters, except for electron density, is insignificant.

In order to gain intuition into the changes of the plasma channel caused by the altered air humidity, in Fig. 4 we show the spatial distribution of the electron density for 50 μJ UV laser pulses for RH = 0 and 100%. We see that in more humid air the plasma channel becomes longer and wider, its peak electron density rises, and the total plasma volume becomes larger.

Another interesting result, which we can extract from the simulations, is the percentage of total electrons generated by ionization of individual air components. For example, for dry air with zero RH, ionization of oxygen gives 65.2% of all plasma electrons, while the rest 34.8% of electrons comes from ionized nitrogen. However, already for RH = 10% (only 0.23% of water molecules in air) the amount of electrons generated through ionization of water vapor reaches 61.6% (the ratio of electrons produced from O_2 and N_2 remains the same). For RH = 50% (1.15% of water molecules in air) the percent of electrons coming from ionized water vapor becomes 89%. And finally, when RH reaches 100% (2.31% of water molecules in air) we see that almost all electrons in the plasma channel (≈94%) are produced due to ionization of water molecules. Thus, most of the ions in air plasma produced by UV laser pulses are expected to be water ions and/or their derivatives. Therefore, in order to describe the evolution of such plasma the existing photochemical models (e.g., [9,28]) will require an update.

In conclusion, we studied, both experimentally and numerically, the influence of air humidity on the filamentation of UV laser pulses with 248 nm wavelength. We demonstrated that the presence of water vapor in air leads to a significant increase (up to one order of magnitude) of the peak electron density and total amount of electrons in plasma channels produced by UV laser pulses. We also found that the plasma channels in humid air, compared with those in dry air, become longer and wider. From our simulations we have seen that with growth of the relative humidity, the peak intensity and peak fluence inside the filament decrease while the losses of laser energy, in opposite, increase. At the same time, we did not find any effect of air humidity on filamentation of NIR laser pulses with 744 nm wavelength. These findings can have considerable impact in all atmospheric applications of filaments, including lightning and weather control as well as in free space telecommunications.

Funding. Russian Foundation for Basic Research (RFBR) (17-02-00722, 18-32-00726); Qatar Foundation (NPRP9-383-1-083); Horizon 2020 Framework Programme (H2020) (EC-GA 654148).

REFERENCES

1. A. Couairon and A. Mysyrowicz, Phys. Rep. **441**, 47 (2007).
2. T. Löffler, M. Kress, M. Thomson, and H. G. Roskos, Acta Phys. Pol. A **107**, 99 (2005).
3. J.-P. Wolf, Rep. Prog. Phys. **81**, 026001 (2018).
4. I. Dey, K. Jana, V. Y. Fedorov, A. D. Koulouklidis, A. Mondal, M. Shaikh, D. Sarkar, A. D. Lad, S. Tzortzakis, A. Couairon, and G. R. Kumar, Nat. Commun. **8**, 1184 (2017).
5. B. Shim, S. E. Schrauth, and A. L. Gaeta, Opt. Express **19**, 9118 (2011).
6. T.-J. Wang, H. Xu, J.-F. Daigle, A. Sridharan, S. Yuan, and S. L. Chin, Opt. Lett. **37**, 1706 (2012).
7. S. Yuan, T. Wang, P. Lu, S. L. Chin, and H. Zeng, Appl. Phys. Lett. **104**, 091113 (2014).
8. H. Li, Y. Jiang, S. Li, A. Chen, S. Li, and M. Jin, Chem. Phys. Lett. **662**, 188 (2016).
9. K. Yoshihara, Chem. Lett. **34**, 1370 (2005).
10. P. Rohwetter, J. Kasparian, K. Stelmaszczyk, Z. Hao, S. Henin, N. Lascoux, W. Nakaema, Y. Petit, M. Queißer, R. Salamé, E. Salmon, L. Wöste, and J.-P. Wolf, Nat. Photonics **4**, 451 (2010).
11. Y. Petit, S. Henin, J. Kasparian, and J.-P. Wolf, Appl. Phys. Lett. **97**, 021108 (2010).
12. L. de la Cruz, E. Schubert, D. Mongin, S. Klingebiel, M. Schultze, T. Metzger, K. Michel, J. Kasparian, and J.-P. Wolf, Appl. Phys. Lett. **109**, 251105 (2016).
13. G. Schimmel, T. Produit, D. Mongin, J. Kasparian, and J.-P. Wolf, Optica **5**, 1338 (2018).
14. S. Yuan, T. Wang, Y. Teranishi, A. Sridharan, S. H. Lin, H. Zeng, and S. L. Chin, Appl. Phys. Lett. **102**, 224102 (2013).
15. A. V. Shutov, N. N. Ustinovskii, I. V. Smetanin, D. V. Mokrousova, S. A. Goncharov, S. V. Ryabchuk, E. S. Sunchugasheva, L. V. Seleznev, A. A. Ionin, and V. D. Zvorykin, Appl. Phys. Lett. **111**, 224104 (2017).
16. A. V. Shutov, N. N. Ustinovskii, I. V. Smetanin, D. V. Mokrousova, S. A. Goncharov, S. V. Ryabchuk, E. S. Sunchugasheva, L. V. Seleznev, A. A. Ionin, and V. D. Zvorykin, Appl. Phys. Lett. **113**, 189902 (2018).
17. J. Schwarz, P. Rambo, J. C. Diels, M. Kolesik, E. M. Wright, and J. V. Moloney, Opt. Commun. **180**, 383 (2000).
18. S. Tzortzakis, B. Lamouroux, A. Chiron, M. Franco, B. Prade, A. Mysyrowicz, and S. D. Moustaizis, Opt. Lett. **25**, 1270 (2000).
19. A. Couairon and L. Berge, Phys. Rev. Lett. **88**, 135003 (2002).
20. I. V. Smetanin, A. O. Levchenko, A. V. Shutov, N. N. Ustinovskii, and V. D. Zvorykin, Nucl. Instrum. Methods Phys. Res., Sect. B **369**, 87 (2016).
21. D. E. Shipilo, N. A. Panov, E. S. Sunchugasheva, D. V. Mokrousova, A. V. Shutov, V. D. Zvorykin, N. N. Ustinovskii, L. V. Seleznev, A. B. Savel'ev, O. G. Kosareva, S. L. Chin, and A. A. Ionin, Opt. Express **25**, 25386 (2017).
22. D. Abdollahpour, S. Suntsov, D. G. Papazoglou, and S. Tzortzakis, Opt. Express **19**, 16866 (2011).
23. Laser Quantum, "vCHIRP," https://www.laserquantum.com/products/detail.cfm?id=82.
24. A. Couairon, E. Brambilla, T. Corti, D. Majus, O. Ramírez-Góngora, and M. Kolesik, Eur. Phys. J. Spec. Top. **199**, 5 (2011).
25. E. R. Peck and K. Reeder, J. Opt. Soc. Am. **62**, 958 (1972).
26. M. Mlejnek, E. M. Wright, and J. V. Moloney, Opt. Lett. **23**, 382 (1998).
27. A. L. Buck, J. Appl. Meteorol. **20**, 1527 (1981).
28. N. L. Aleksandrov, S. B. Bodrov, M. V. Tsarev, A. A. Murzanev, Y. A. Sergeev, Y. A. Malkov, and A. N. Stepanov, Phys. Rev. E **94**, 013204 (2016).